EurJIC European Journal of Inorganic Chemistry

ChemPubSoc Europe

Photolysis of Selenoacetic Acids

J. A. Gómez Castaño, R. M. Romano,* H. Beckers, H. Willner, C. O. Della Védova

Formation of the Matrix-Isolated Difluoromethylselanes XCF_2SeH (X = H, Cl) Through Photolysis of Selenoacetic Acids, $XCF_2C(O)SeH$

Keywords: Matrix isolation / Photochemistry / Vibrational spectroscopy / Density functional calculations / Selenium / Selanes

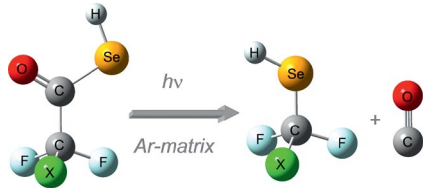

Matrix photochemistry has been successfully employed for the formation of two hitherto unknown selane molecules, HCF_2SeH and $ClCF_2SeH$, by starting from $HCF_2C(O)SeH$ and $ClCF_2C(O)SeH$ acids. The species were identified through their IR spectra, with the assistance of ab initio and DFT methods.

EurJIC European Journal of Inorganic Chemistry

www.eurjic.org FULL PAPER

DOI:10.1002/ejic.201300322

Formation of the Matrix-Isolated Difluoromethylselanes XCF_2SeH (X = H, Cl) Through Photolysis of Selenoacetic Acids, $XCF_2C(O)SeH$

Jovanny A. Gómez Castaño,[a][‡] Rosana M. Romano,*[a] Helmut Beckers,[b] Helge Willner,[b] and Carlos O. Della Védova[a]

Keywords: Matrix isolation / Photochemistry / Vibrational spectroscopy / Density functional calculations / Selenium / Selanes

Two hitherto unknown difluoromethylselanes, HCF_2SeH and $ClCF_2SeH$, were formed by photolysis of difluoroselenoacetic and chlorodifluoroselenoacetic acids isolated in solid argon. The progress of the photolysis was monitored by FTIR spectroscopy. The photoproducts were identified by comparison of experimental with theoretically predicted spectra and reported spectra for known species. The photochemical decomposition mechanisms of $HCF_2C(O)SeH$ and $ClCF_2C(O)SeH$ is presented.

Introduction

Photolysis of matrix-isolated species has been shown to be a useful technique for the formation of new compounds.[1] The low temperatures and high dilutions prevent all photochemical pathways other than unimolecular ones. This technique is most relevant for the formation of unstable and reactive species. The stabilization of molecular complexes is also favored by the rigid environment of the matrix, transforming this technique into a valuable tool for the study of molecular adducts or complexes.[2]

In recent years, we have pursued new matrix-isolated species using two different strategies. (i) Unstable small molecules have been obtained from the photolysis of matrix-isolated precursors. For example, BrSCl[3] and CH_3SF,[4] isolated in inert matrixes, were obtained from the UV/Vis broad-band photolysis of ClC(O)SBr and $FC(O)SCH_3$, respectively. Moreover, during the photolysis of ClC(O)SBr the bond isomer BrC(O)SCl was also observed among other photoproducts. This result is related to the recently reported isotopic scrambling in CD_3CHO by photolysis.[5] (ii) Reactions in matrices have been extensively used for the formation of new families of compounds (see for example ref.[6] and references cited therein).

The photolysis of selenoacetic acid in its normal and perdeuterated forms, $CH_3C(O)SeH$ and $CD_3C(O)SeD$,[7] and of trifluoroselenoacetic acid, $CF_3C(O)SeH$,[8] isolated in solid inert matrices resulted in the formation of the corresponding methylselanes, CH_3SeH, CD_3SeD, and CF_3SeH, together with other photoproducts. In this study we present the matrix-isolated photochemistry of two selenoacetic acids recently reported, $HCF_2C(O)SeH$ and $ClCF_2C(O)SeH$.[9] The main objective of this work was the formation of the two hitherto unknown difluoromethylselanes, HCF_2SeH and $ClCF_2SeH$, and elucidation of the photochemical mechanisms.

Results and Discussion

Photolysis of Matrix-Isolated Difluoroselenoacetic Acid

The IR spectra of matrix-isolated difluoroselenoacetic acid have been recently described,[9] and interpreted in terms of an equilibrium of *syn–gauche* and *anti–syn* conformers, in accordance with the predictions of theoretical calculations. In this work, a sample of $HCF_2C(O)SeH$ isolated in an Ar matrix at 15 K was exposed to light of different energies. When the output of the lamp was limited to $\lambda \geq 420$, 375, 360, 320, or 305 nm no changes were observed in the IR spectra of the irradiated matrix. This behavior is in accordance with the UV/Vis spectrum of gaseous $HCF_2C(O)SeH$, which presents an absorption centered at 252 nm.[9]

[a] CEQUINOR (UNLP-CONICET), Departamento de Química, Facultad de Ciencias Exactas, Universidad Nacional de La Plata,
47 esq. 115, 1900 La Plata, Argentina
E-mail: romano@quimica.unlp.edu.ar
Homepage: http://cequinor.quimica.unlp.edu.ar/
[b] Anorganische Chemie, Bergische Universität Wuppertal, Gaußstr. 20, 42097 Wuppertal, Germany
[‡] Present address: Escuela de Ciencias Químicas, Facultad de Ciencias, Universidad Pedagógica y Tecnológica de Colombia (UPTC),
Avenida Central del Norte, 150003 Tunja, Boyacá, Colombia

Supporting information for this article is available on the WWW under http://dx.doi.org/10.1002/ejic.201300322

The matrix was then exposed to light of $\lambda \geq 280$ nm for different irradiation times. As a consequence of the photolysis, the intensity of the IR absorptions corresponding to $HCF_2C(O)SeH$ decreased, while several new bands developed in the spectrum. Later, the matrix was irradiated with unfiltered light ($\lambda \geq 200$ nm) from a high-pressure mercury lamp. In these experiments the acid was depleted almost completely, and the photolysis rate was notably increased. New absorptions were detected in the IR spectra of the irradiated matrices. To identify the species formed on photolysis, we have taken into account their distinctive behavior as a function of irradiation time.

The IR band that developed in the region of 2140 cm^{-1} was readily assigned to the formation of the CO molecule.[10,11] As depicted in Figure 1, two absorptions at 2139.6 and 2144.1 cm^{-1} were observed. These two features arise from different species, as can be clearly seen in Figure 2, which depicts the variation in intensity of the IR bands with irradiation time. The bands at 2332.3 and 2328.1 cm^{-1} (Figure 3) are attributed to the formation of H_2Se, in accordance with the reported values for H_2Se isolated in Ar matrix.[12]

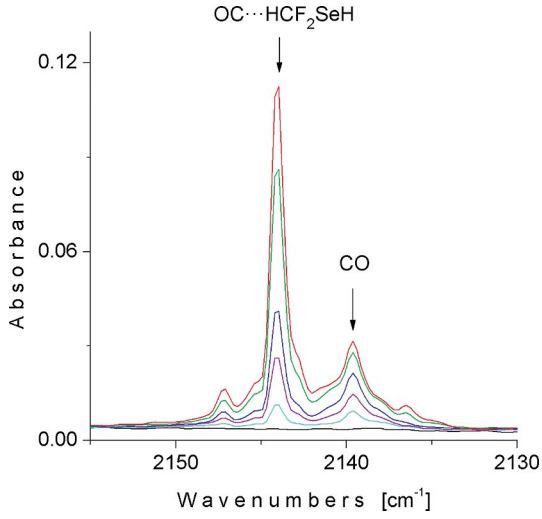

Figure 1. IR spectra between 2130 and 2155 cm^{-1} of an Ar matrix initially containing $HCF_2C(O)SeH$ recorded at different times during irradiation: after 0 (black), 5 (sky-blue), 15 (magenta), and 30 min (blue) irradiation with $\lambda \geq 280$ nm, and subsequently after 3 (green) and 5 min (red) further irradiation with $\lambda \geq 200$ nm.

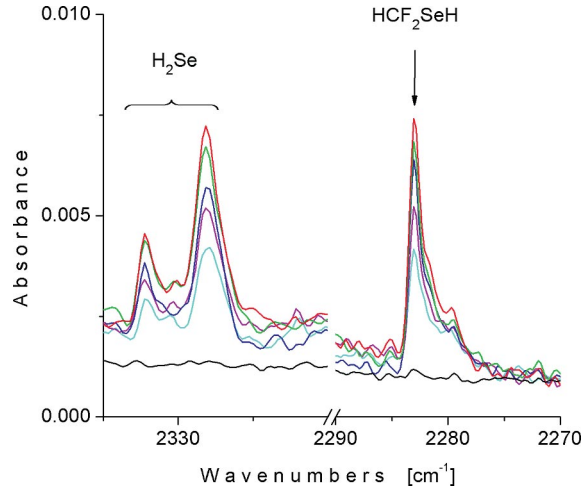

Figure 3. IR spectra between 2270 and 2335 cm^{-1} of an Ar matrix initially containing $HCF_2C(O)SeH$, recorded at different times during irradiation: after 0 (black), 5 (sky-blue), 15 (magenta), and 30 min (blue) irradiation with $\lambda \geq 280$ nm, and subsequently after 3 (green) and 5 min (red) irradiation with $\lambda \geq 200$ nm.

A group of bands located at 3001.4, 2283.0, 1311.7, 1282.6, 1082.1, 1081.1, 1078.3, 595.8 and 547.8 cm^{-1} follows the same pattern of behavior with irradiation time as the CO absorption at 2144.1 cm^{-1} in Figure 2. Taking into consideration the reported photochemical formation of CH_3SeH[7] and CF_3SeH[8] from matrix-isolated $CH_3C(O)SeH$ and $CF_3C(O)SeH$, respectively, the new group of bands are attributed to difluoromethylselane, HCF_2SeH. As far as we know, there is no report of this species in the

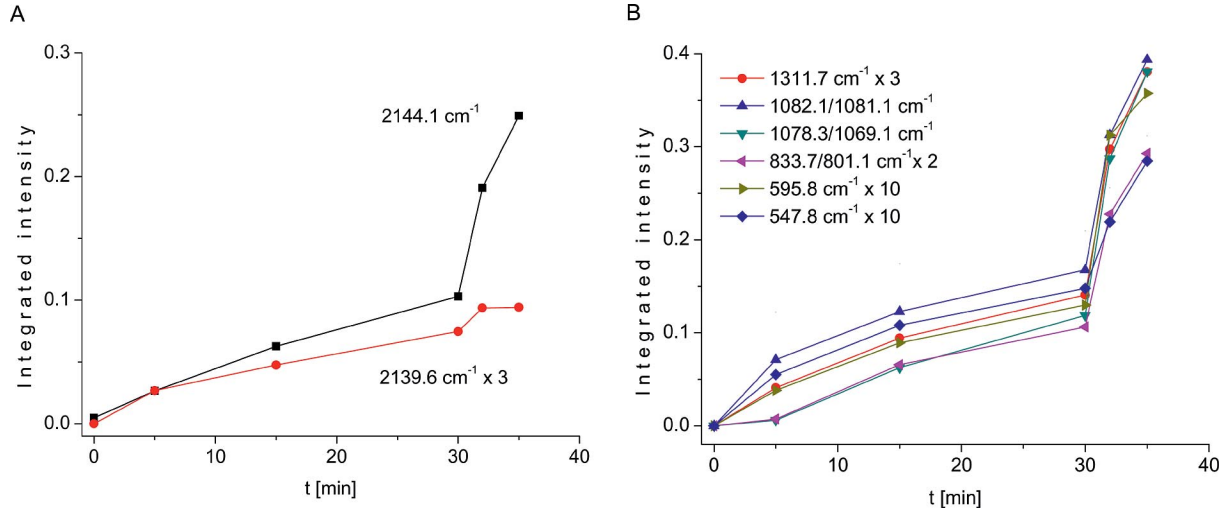

Figure 2. Plot of the intensities of the Ar-matrix IR bands of (A) CO and (B) HCF_2SeH vs irradiation time, upon irradiation with light of $\lambda \geq 280$ nm for 30 min followed by irradiation with light of $\lambda \geq 200$ nm.

literature. This assignment is supported by a very good agreement between the experimental and theoretically predicted IR spectra (see the Theoretical Calculations section). Figures 3, 4, and 5 present three different regions of the IR spectra before and after irradiation of the matrix, where the development of the absorptions assigned to HCF_2SeH can be observed.

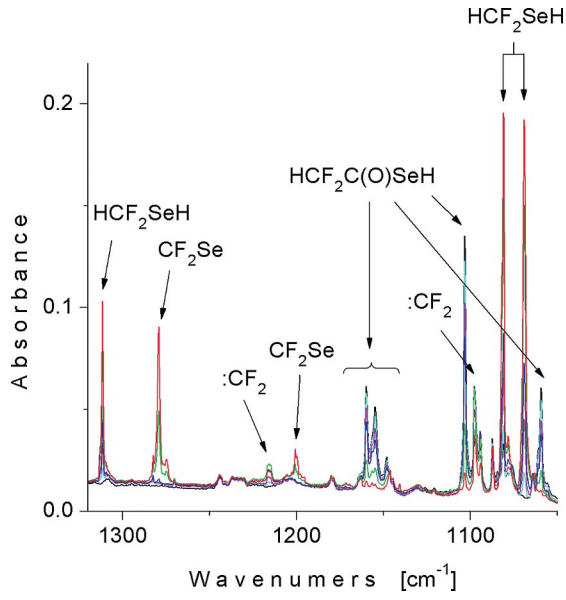

Figure 4. IR spectra between 1050 and 1350 cm^{-1} of an Ar matrix initially containing $HCF_2C(O)SeH$, recorded at different times during irradiation: after 0 (black), 5 (sky-blue), 15 (magenta), and 30 min (blue) irradiation with $\lambda \geq 280$ nm, and subsequently after 3 (green) and 5 min (red) irradiation with $\lambda \geq 200$ nm.

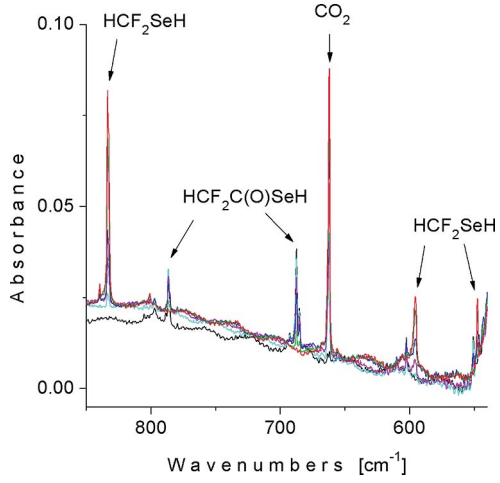

Figure5. IR spectra between 500 and 850 cm^{-1} of an Ar matrix initially containing $HCF_2C(O)SeH$, recorded at different times during irradiation: after 0 (black), 5 (sky-blue), 15 (magenta), and 30 min (blue) irradiation with $\lambda \geq 280$ nm, and subsequently after 3 (green) and 5 min (red) irradiation with $\lambda \geq 200$ nm.

The 2144.1 cm^{-1} IR absorption was assigned to a OC···$HSeCF_2H$ complex [Equation (1)] because its photolytic behavior was similar to that observed for the bands assigned to HCF_2SeH (see Figure 2).

$$HCF_2C(O)SeH \xrightarrow[\lambda \geq 280\ nm]{\text{Ar matrix, 15 K}} HCF_2SeH + CO \quad (1)$$

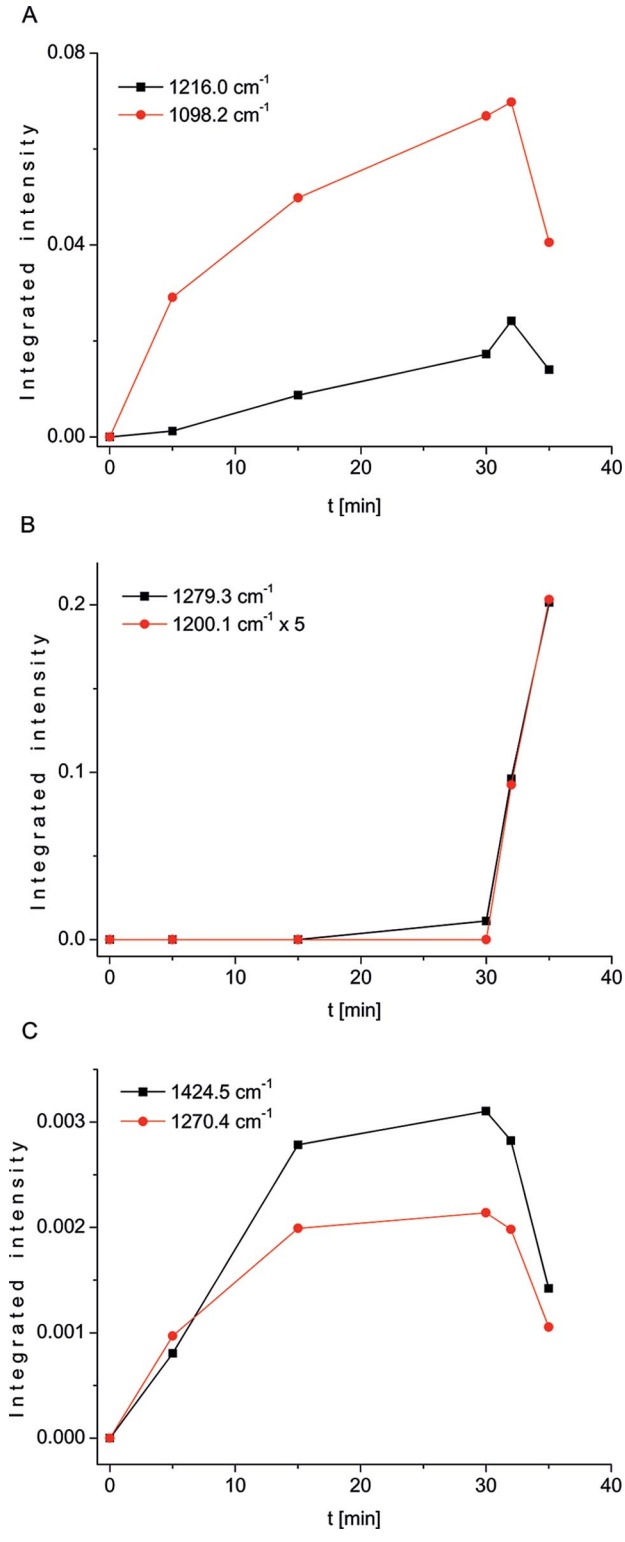

Figure 6. Plot of the intensities of the IR bands assigned to (A) CF_2, (B) CF_2=Se, and (C) CF_2=C=O in an Ar matrix initially containing difluoroselenoacetic acid vs irradiation time, upon irradiation with light of $\lambda \geq 280$ nm for 30 min, followed by irradiation with light of $\lambda \geq 200$ nm.

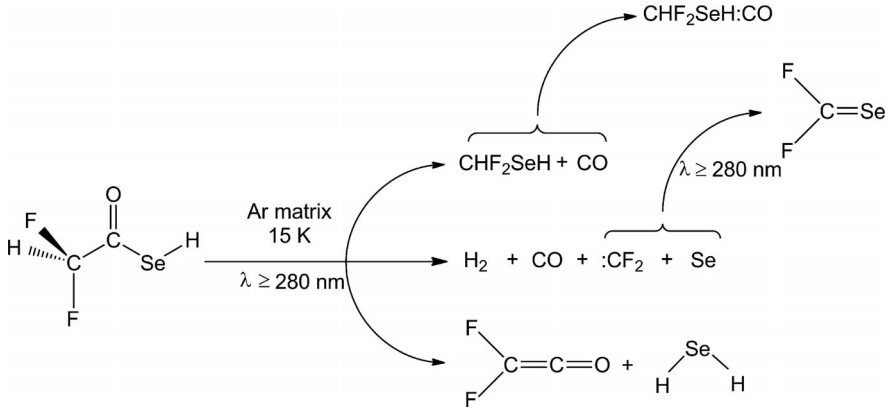

Figure 7. Proposed photochemical decomposition pathways of $HCF_2C(O)SeH$ isolated in an Ar matrix.

Besides the features assigned to HCF_2SeH, Figure 4 also shows the photolytic development of other IR absorption bands at 1279.3, 1216.0, 1200.1, and 1198.2 cm^{-1} upon photolysis. The bands at 1216.0 and 1198.2 cm^{-1} revealed a time-dependent behavior characteristic for an intermediate photoproduct (Figure 6). They were assigned to difluorocarbene, by comparison with reported values.[13] The absorptions at 1279.3 and 1200.1 cm^{-1} seem to be formed at the expense of difluorocarbene (Figure 6), and were attributed to $F_2C{=}Se$, in accordance with its reported IR bands in an Ar matrix.[14] Two extremely weak IR features appearing at 1424.5 and 1270.4 cm^{-1}, that follow a distinct time-dependence, were assigned to fluoroketene, $CF_2C{=}O$.[15] Table 1 includes all wavenumbers observed in the IR spectra of $HCF_2C(O)SeH$ isolated in an Ar matrix after irradiation, together with the reported values for known species, and calculated frequencies for HCF_2SeH.

Table 1. Wavenumbers and assignments of the IR absorptions appearing on photolysis of $HCF_2C(O)SeH$ isolated in an Ar matrix.

ν [cm^{-1}]	Species	Vibrational mode	Wavenumbers reported previously
3001.4	HCF_2SeH	ν (C–H)	3105.8[a]
2332.3, 2328.1	H_2Se	ν (Se–H)	2344[14]
2283.0	HCF_2SeH	ν (Se–H)	2368.9[a]
2144.1	$OC{\cdots}HCF_2SeH$	ν (CO)	–
2139.6	CO	ν (CO)	2138.0[12]
1424.5	$CF_2C{=}O$	ν_{as} CCO	1426.8[17]
1311.7	HCF_2SeH	δ (HCSe)	1326.7[a]
1279.3	CF_2Se	ν_s (CF_2)	1275.0[16]
1270.4	$CF_2C{=}O$	ν_{as} (CF_2)	1274.4[17]
1216.0	$:CF_2$	ν_s (CF_2)	1222[15]
1200.1	CF_2Se	ν_{as} (CF_2)	1196.0[16]
1098.2	$:CF_2$	ν_{as} (CF_2)	1102[15]
1082.1, 1081.1	HCF_2SeH	ν_s (CF_2)	1076.1[a]
1078.3, 1069.1	HCF_2SeH	ν_{as} (CF_2)	1049.0[a]
833.7, 801.1	HCF_2SeH	δ (HSeC)	839.9[a]
595.8	HCF_2SeH	ν (C–Se)	589.1[a]
547.8	HCF_2SeH	δ (CF_2)	539.4[a]

[a] Theoretical wavenumbers calculated for *anti*-HCF_2SeH with the B3LYP/6-311++G** approximation.

On the basis of the experimental findings described above, we propose the photochemical pathways depicted in Figure 7. When an argon matrix containing $HCF_2C(O)SeH$ was irradiated with light of $\lambda \geq 280$ nm, the major photochemical pathway was the elimination of CO and the concomitant formation of the hitherto unknown selane HCF_2SeH. Another photochemical pathway yielded fluorocarbene, while in a third mechanism the removal of the hydrogen atom from the difluoromethyl group gave rise to fluoroketene. When the energy of the radiation was extended to $\lambda \geq 200$ nm, the parent acid was almost completely depleted. Besides the photochemical pathway described above, difluoroselenophosgene, $F_2C{=}Se$, was formed, presumably from the reaction of fluorocarbene with Se atoms.

Photolysis of Matrix-Isolated Chlorodifluoroselenoacetic Acid

The IR spectrum of $ClCF_2C(O)SeH$ isolated in an Ar matrix after deposition reveals the presence of three different conformers, *syn–gauche*, *anti–gauche*, and *anti–syn*. This assignment was previously proposed, and confirmed by the variation of the relative intensity of the bands assigned to each conformer with the deposition temperature.[9]

The matrix was exposed to light in the ranges $\lambda \geq 420$, 360, 320, and 280 nm, and the changes upon photolysis were followed by IR spectroscopy over time. $ClCF_2C(O)SeH$ isolated in an Ar matrix proved photochemically stable when

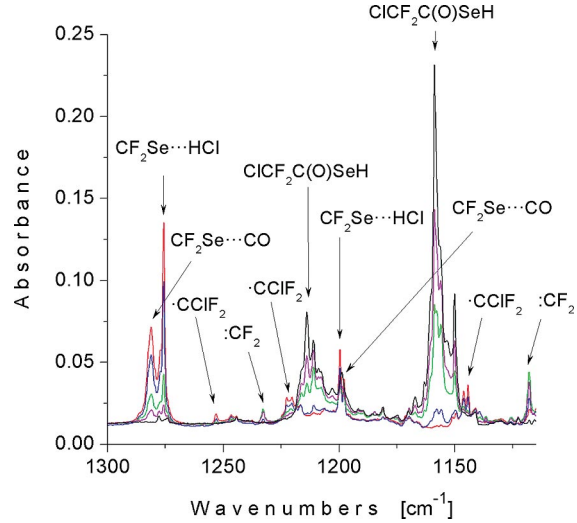

Figure 8. IR spectra between 1115 and 1300 cm^{-1} of an Ar matrix initially containing $ClCF_2C(O)SeH$, recorded at different times during irradiation ($\lambda \geq 280$ nm): after 0 (black), 0.5 (magenta), 1 (green), 3 (blue), and 6 min (red) irradiation.

irradiated with light in the range of $\lambda \geq 420$ nm. When the wavelength was reduced to 280 nm, development of several new products was observed, together with the almost total depletion of the starting acid, as depicted in Figure 8. When filters were used to cut the energy of the light ($\lambda \geq 360$ and 320 nm), far fewer photoproducts were obtained. To help in the assignment of the IR absorptions to the photoproducts, the integrated intensity of the new IR signals was plotted against the irradiation time, and the bands were grouped together according to their photolytic behavior (see Figure 9).

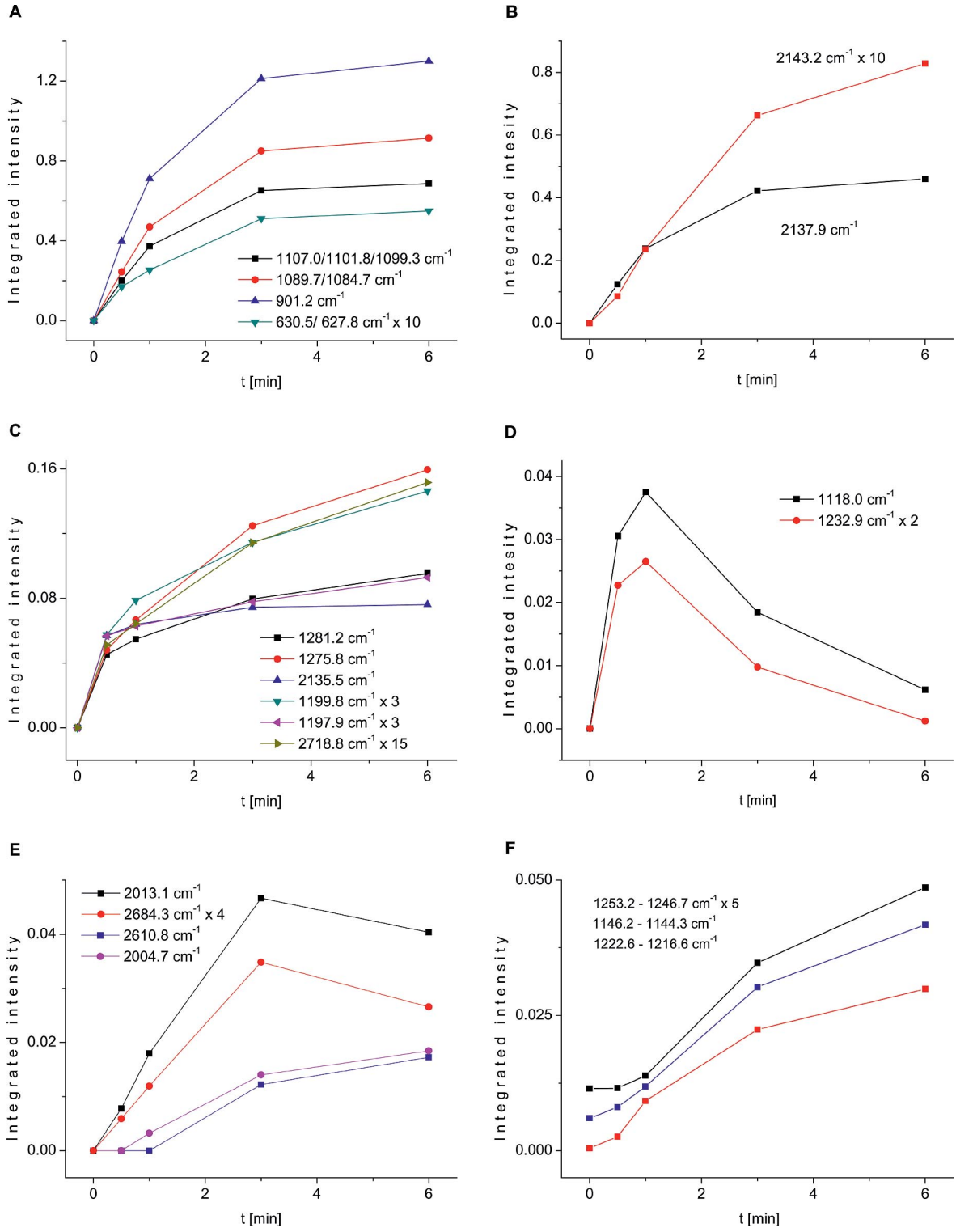

Figure 9. Plot of the intensities of the IR bands assigned to (A) $ClCF_2SeH$, (B) CO, (C) CF_2Se:CO and CF_2Se:HCl complexes, (D) :CF_2, (E) OCSe:HCl complex, and (F) radical $^{\cdot}ClCF_2$ in an Ar matrix initially containing chlorodifluoroselenoacetic acid vs irradiation time ($\lambda \geq 280$ nm).

As will be discussed, some of the products that developed on photolysis appear to be perturbed by the presence of other photoproducts in the same matrix cage. In order to better understand the spectra, we heated $ClCH_2C(O)SeH$/Ar at 210 °C in the spray nozzle before matrix deposition. In contrast to photolysis experiments, after pyrolysis only monomeric species were deposited.

Figure 10 presents IR spectra, in the spectral region corresponding to the CO molecule, recorded at different times as an Ar matrix initially containing $ClCF_2C(O)SeH$ is irradiated. Several features with a complicated pattern developed in this region, suggesting complex formation between CO and different products. The most intense of these absorptions, at 2137.9 cm^{-1}, is assigned to the monomeric CO molecule, by comparison with the reported value.[10] The other bands at 2154.3, 2143.2, and 2135.5 cm^{-1} will be discussed below, after the identification of the other photoproducts.

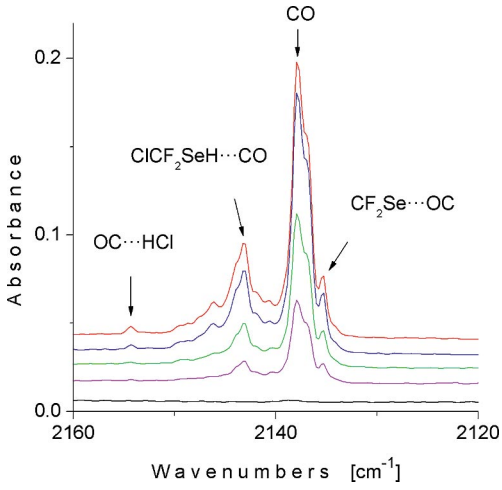

Figure 10. IR spectra between 2120 and 2160 cm^{-1} of an Ar matrix initially containing $ClCF_2C(O)SeH$, recorded at different times during irradiation ($\lambda \geq 280$ nm): after 0 (black), 0.5 (magenta), 1 (green), 3 (blue), and 6 min (red) irradiation.

A group of absorptions at 1107.0/1101.8/1099.3, 1089.7/1084.7, 901.2, 748.1, and 630.5/627.8 cm^{-1}, all of which follow the same photolysis pattern, could not be attributed to any known photoproducts. Considering the photolysis mechanisms reported for $CH_3C(O)SeH$[7] and $CF_3C(O)SeH$[8] isolated in a solid argon matrix, and also the photochemical study of $HCF_2C(O)SeH$ presented above in this paper, we looked at the formation of $ClCF_2SeH$. The predicted fundamental vibrations and intensities for $ClCF_2SeH$ (see Theoretical Calculations section) are in agreement with the observed features, as shown in Figure 11.

The features observed at 1253.2/1246.7, 1222.6/1220.4/1218.5/1216.6, and 1146.2/1144.3 cm^{-1} (Figure 8) were suggested to arise from the $\cdot ClCF_2$ radical, on the basis of reported values for this species isolated in Ar matrix.[16] The difluorocarbene $:CF_2$ was also identified by the IR absorptions at 1232.9 and 1118.0 cm^{-1}, close to the literature values.[13] The behavior of these bands over time as irradiation proceeds is depicted in Figure 9 (D), and is characteristic

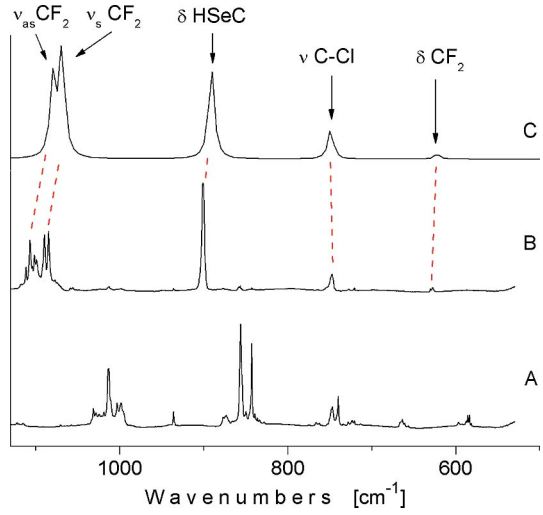

Figure 11. IR spectra between 500 and 1300 cm^{-1}: (A) recorded for an Ar matrix initially containing $ClCF_2C(O)SeH$ immediately after deposition; (B) as for (A), but after 4 min of photolysis with light of $\lambda \geq 280$ nm; (C) simulated for *anti*-$ClCF_2SeH$ using the B3LYP/6-311++G** approximation.

of an intermediate product, consistent with the high reactivity of this species.

The bands appearing at 1281.2, 1275.8, 1199.8, and 1197.9 cm^{-1} may be attributed to difluoroselenophosgene, $F_2C{=}Se$ (see Figure 8). These wavenumbers are very close to the reported values (1275.0 and 1196.0 cm^{-1})[14] and those we obtained by thermolysis at 210 °C of $ClCF_2C(O)SeH$ isolated in Ar matrix, 1274.3 and 1195.2 cm^{-1}.[9] A small shift to higher wavenumbers is probably due to complex formation in the matrix cage with other photoproducts. Figure 9 (C) shows the behavior of the bands assigned to $F_2C{=}Se$ plotted against the irradiation time, together with absorptions that appear at 2135.5 cm^{-1} (see Figure 10) and 2718.8 cm^{-1} (Figure 12), which correspond to CO and HCl, respectively. The similarity in the photolysis behavior of

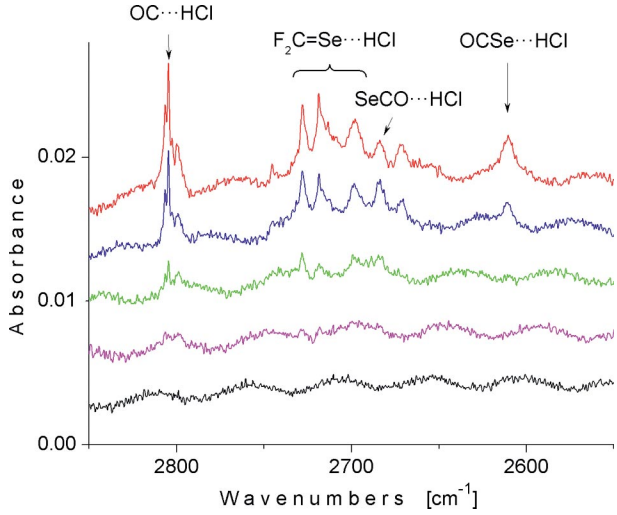

Figure 12. IR spectra between 2550 and 2850 cm^{-1} of an Ar matrix initially containing $ClCF_2C(O)SeH$, recorded at different times during irradiation ($\lambda \geq 280$ nm): after 0 (black), 0.5 (magenta), 1 (green), 3 (blue), and 6 min (red) irradiation.

these IR bands is evident from inspection of this plot. The bands at 1275.8 and 1199.8 cm^{-1} follow the same behavior over time as the feature arising from HCl, and are assigned to a complex, F_2C=Se···HCl. A similar complex between H_2C=S and HCl, was reported in the photolysis of ClC(O)SCH_3 isolated in an Ar matrix.[17] The bands at 1281.2, 1197.9, and 2135.5 cm^{-1} were attributed to a F_2C=Se···OC molecular complex, as indicated in Figure 9 (C).

The bands at 2806.8 and 2154.3 cm^{-1} were assigned to a linear OC···HCl adduct in accordance with the literature values.[18–20] Wavenumber shifts of –72.8 cm^{-1} for the HCl subunit and of +16.3 cm^{-1} for the CO fragment have been reported for this complex isolated in an Ar matrix,[19] in good agreement with the observed shifts of –81.2 and +16.3 cm^{-1}.

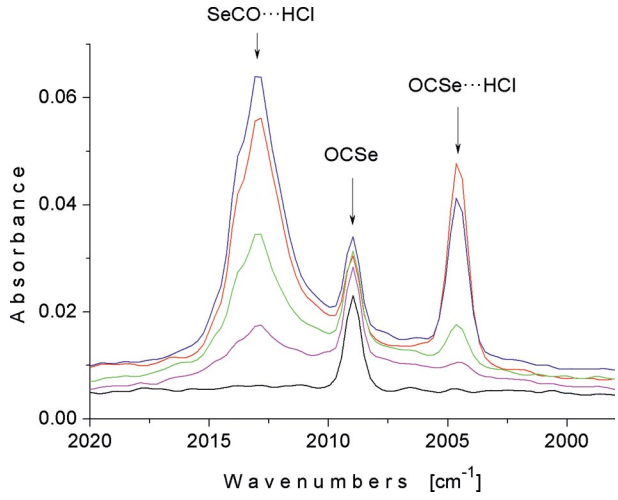

Figure 13. IR spectra between 2020 and 1995 cm^{-1} of an Ar matrix initially containing $ClCF_2C(O)SeH$, recorded at different times during irradiation ($\lambda \geq 280$ nm): after 0 (black), 0.5 (magenta), 1 (green), 3 (blue), and 6 min (red) irradiation.

Table 2. Wavenumbers and assignments of the IR absorption bands appearing on photolysis of $ClCF_2C(O)SeH$ isolated in an Ar matrix.

ν [cm^{-1}]	Species	Vibrational mode	Wavenumbers reported previously
2806.8, 2804.8	OC···HCl	ν (H–Cl)	2815.2,[19] 2818[10]
2728.1, 2718.8, 2698.4	F_2CSe···HCl	ν (H–Cl)	–
2684.3, 2671.9	SeCO···HCl	ν (H–Cl)	–
2610.8	OCSe···HCl	ν (H–Cl)	–
2154.3	OC···HCl	ν(CO)	2154.3[19]
2143.2	$ClCF_2SeH$···CO	ν(CO)	–
2137.9	CO	ν(CO)	2138.0[10]
2135.5	CF_2Se···OC	ν(CO)	–
2013.1	SeCO···HCl	ν(CO)	–
2009.0	OCSe	ν(CO)	2009.0[6]
2004.7	OCSe···HCl	ν(CO)	–
1281.2	CF_2Se···OC	$\nu_s(CF_2)$	–
1275.8	F_2CSe···HCl	$\nu_s(CF_2)$	–
1274.3	CF_2Se	$\nu_s(CF_2)$	1275.0[14]
1253.2, 1246.7	$^{\cdot}ClCF_2$		1253, 1249[16]
1232.9	$:CF_2$	$\nu_s(CF_2)$	1222[13]
1222.6, 1220.4, 1218.5, 1216.6	$^{\cdot}ClCF_2$		1208[16]
1199.8	F_2CSe···HCl	$\nu_{as}(CF_2)$	–
1197.9	CF_2Se···OC	$\nu_{as}(CF_2)$	–
1195.2	CF_2Se	$\nu_{as}(CF_2)$	1196.0[14]
1146.2, 1144.3	$^{\cdot}ClCF_2$		1148.2, 1146.6[16]
1118.0	$:CF_2$	$\nu_{as}(CF_2)$	1102.0[13]
1112.0, 1107.0, 1101.8, 1099.6	$ClCF_2SeH$	$\nu_{as}(CF_2)$	1079.5[a]
1089.7, 1084.7	$ClCF_2SeH$	$\nu_s(CF_2)$	1068.9[a]
901.2	$ClCF_2SeH$	δ(HSeC)	891.2[a]
748.1	$ClCF_2SeH$	ν_s(CCl)	749.2[a]
630.5, 627.8	$ClCF_2SeH$	$\delta(CF_2)$	622.6[a]

[a] Theoretical wavenumbers calculated for *anti*-$ClCF_2SeH$ with the B3LYP/6-311++G** approximation.

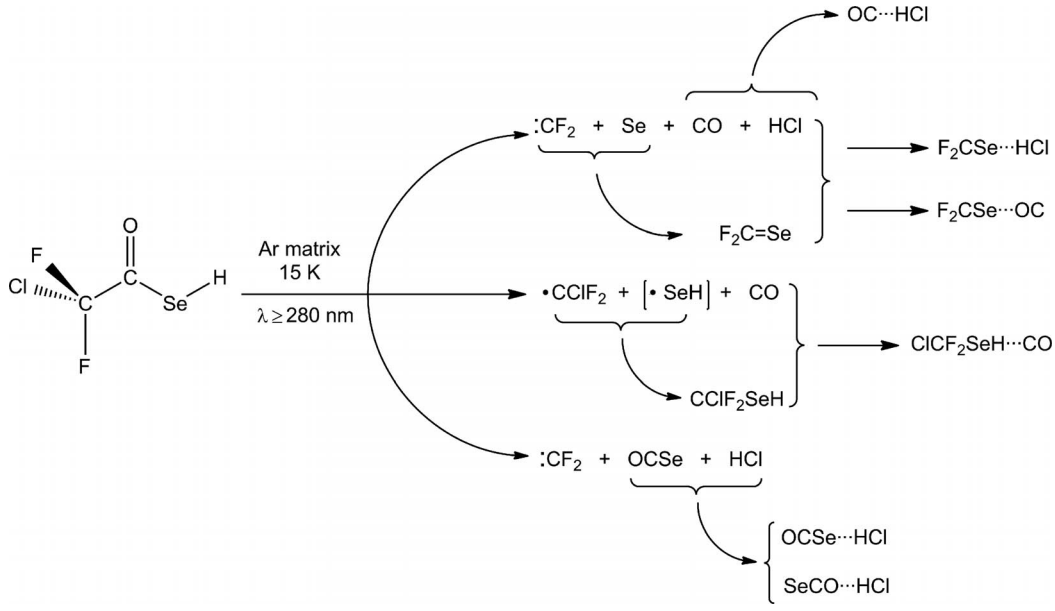

Figure 14. Proposed photochemical decomposition pathways of $ClCF_2C(O)SeH$ isolated in an Ar matrix.

As can be seen in Figure 9 (B), the photolytic behavior of the absorption at 2143.2 cm^{-1}, depicted in Figure 10, is similar to that of chlorodifluoromethylselane [Figure 9 (A)]. The blueshift of this CO vibrational stretching mode is then attributed to perturbation of the CO molecule by the presence of $ClCF_2SeH$ in the same matrix site.

Figure 13 shows the new features that develop after photolysis ($\lambda \geq 280$ nm) in the IR spectrum of matrix-isolated $ClCF_2C(O)SeH$ in the spectral region characteristic for the OCSe molecule. The 2009.0 cm^{-1} band of monomeric OCSe[6] is observed in the spectrum recorded immediately after deposition, denoting slight thermal decomposition of the starting compound in the gas phase. The bands at higher (2013.1 cm^{-1}) and lower (2004.7 cm^{-1}) wavenumbers that develop on photolysis indicate the formation of OCSe perturbed by different photofragments. As shown in Figure 9 (E), the behavior of these absorptions allows us to correlate them with the features at 2684.3 and 2610.8 cm^{-1} assigned to perturbed HCl. Two different 1:1 HCl/OCSe molecular complexes are proposed as an explanation of the experimental findings.

Table 2 includes all the IR absorption bands observed on photolysis of $ClCF_2C(O)SeH$ ($\lambda \geq 280$ nm), together with proposed assignments and comparison with reported wavenumbers. A schematic representation of the different photochemical pathways, based on the identification of the photoproducts and their kinetic behavior, is presented in Figure 14. The most important process is the formation of $ClCF_2SeH$ by elimination of CO from the parent acid. An alternative pathway leads to the formation of difluoroselenophosgene, perturbed by the presence of CO or HCl generated in the same matrix cage. A third mechanism produces carbonylselenide, OCSe, presumably complexed with an HCl molecule. Difluorocarbene, CF_2, clearly shows an intermediate behavior, while the chlorodifluoromethyl radical appears as a stable species under these conditions.

Theoretical Calculations

In order to compare the experimental wavenumbers tentatively assigned to HCF_2SeH and $ClCF_2SeH$ in the IR spectra obtained during photolysis of $HCF_2C(O)SeH$ and $ClCF_2C(O)SeH$, respectively, a theoretical study of these two selane molecules was performed.

Initially, the conformational preferences of HCF_2SeH were explored using the B3LYP/6-311++G** level of approximation. Figure 15 shows the potential energy curve as a function of the H–Se–C–H dihedral angle, calculated through a relaxed scan in which the angle was varied from 0° to 180° in steps of 10°. The curve has two minima, at approximately 50° (*gauche*) and 180° (*anti*), that were subsequently fully optimized using the B3LYP/6-311++G** and MP2/6-311++G** theoretical methods. The geometrical parameters are presented in the Supporting Information (Table S1). The energy difference between the *gauche* and *anti* forms, including ZPE corrections, was predicted to be 0.36 (B3LYP/6-311++G**) and 0.65 (MP2/6-311++G**) kcal/mol.

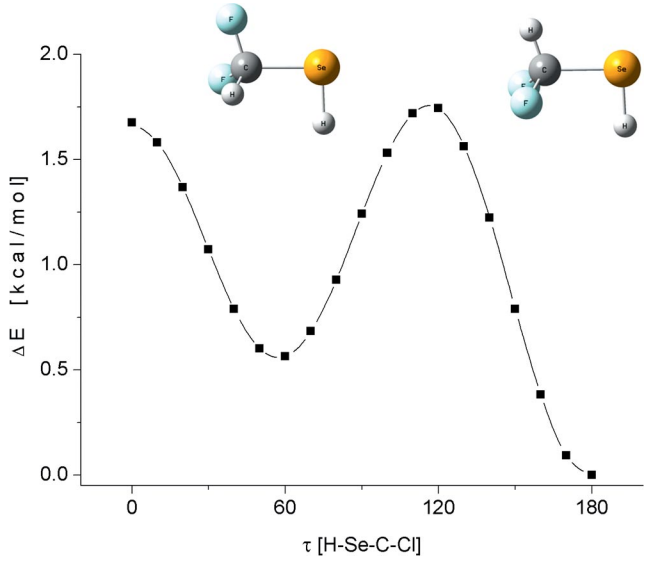

Figure 15. Potential energy curve of HCF_2SeH as a function of the H–Se–C–H dihedral angle calculated with the B3LYP/6-311++G** approximation, and molecular models for the *anti* (right) and *gauche* (left) conformers.

The vibrational frequencies of both forms of HCF_2SeH were calculated to characterize them as true minima, with no imaginary values, and also to compare them with the experimental wavenumbers observed in the photolysis of $HCF_2C(O)SeH$. The complete list of the unscaled theoretical fundamental vibrational modes of HCF_2SeH together with their proposed assignments is presented in the Supplementary Information (Table S2), while Table 1 shows the correlation with the experimental findings.

The theoretical study of $ClCF_2SeH$ was performed similarly. As a starting point, the energy of the system as a function of the Cl–Se–C–H dihedral angle was investigated. The

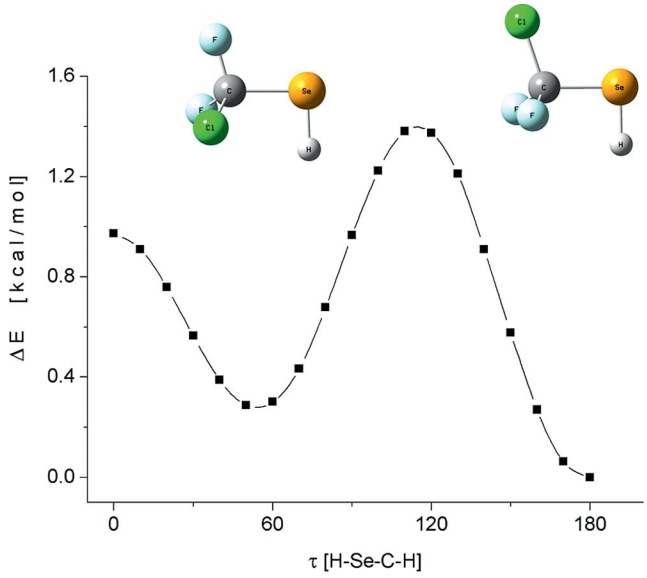

Figure 16. Potential energy curve of $ClCF_2SeH$ as a function of the Cl–Se–C–H dihedral angle calculated using the B3LYP/6-311++G** approximation, and molecular models for the *anti* (right) and *gauche* (left) conformers.

resulting potential energy curve, calculated with the B3LYP/6-311++G** model, has two energy minima, corresponding to the *gauche* and *anti* forms (Figure 16). These two structures were subsequently fully optimized (the geometrical parameters are presented as Supporting Information in Table S3). The energy difference between the *gauche* and *anti* forms, including ZPE corrections, was predicted to be 0.66 (B3LYP/6-311++G**) and 0.69 (MP2/6-311++G**) kcal/mol. The unscaled theoretical fundamental vibrational modes of $ClCF_2SeH$ together with their proposed assignments are presented in the Supplementary Information (Table S4), while Table 2 shows the correlation with the experimental findings.

Conclusions

Matrix photochemistry has been successfully employed for the formation of two hitherto unknown selane molecules, HCF_2SeH and $ClCF_2SeH$, starting from $HCF_2C(O)SeH$ and $ClCF_2C(O)SeH$ acids, respectively. The species were identified through their IR spectra, with the assistance of ab initio and DFT methods.

Mechanisms for the photochemical reactions were proposed by means of following the development of different IR absorption bands on photolysis over time during irradiation. When exposed to light of $\lambda \geq 280$ nm, the principal reaction undergone by both acids leads to formation of the XCF_2SeH species, with X = H, Cl, accompanied by elimination of CO. This mechanism is in agreement with the main photoevolution pathway found for several XC(O)SY compounds in novel gas matrices [for example, the matrix-isolation photochemistry of FC(O)SCl,[21] FC(O)SBr,[22] ClC(O)SBr,[3] $ClC(O)SCH_3$,[17] $FC(O)SCH_3$[4]]. The recently reported photolyses of selenoacetic acid in its normal and perdeuterated forms, $CH_3C(O)SeH$ and $CD_3C(O)SeD$,[7] and of trifluoroselenoacetic acid, $CF_3C(O)SeH$,[8] isolated in solid inert matrices also have the same main mechanism.

A second matrix-photochemical pathway of $HCF_2C(O)SeH$ and $ClCF_2C(O)SeH$ leads to the formation of difluoroselenophosgene, $F_2C{=}Se$. The formation of HCl was clearly observed when $ClCF_2C(O)SeH$ was photolyzed. In contrast, during the irradiation of $HCF_2C(O)SeH$, only $F_2C{=}Se$ and CO were detected, while the two remaining hydrogen atoms, or H_2, cannot be detected by this technique.

Both acids undergo a third photochemical reaction, though the pathway depends on the nature of the X atom of the XCF_2– group. When X is a hydrogen atom, the third mechanism gives rise to difluoroketene, $F_2C{=}C{=}O$. A similar pathway was previously reported for species containing the $CH_3C(O)$– group. The formation of ketene was proposed in the UV photolysis of acetone vapor,[23,24] and also in the matrix photochemistry of $CH_3C(O)SH$, $CH_3C(O)SCH_3$, and $CH_3C(O)SC(O)CH_3$.[25] A recent study on the photodissociation of gaseous $CH_3C(O)SH$ has also revealed that the photolysis proceeds according to these same three mechanisms.[26] However, if X is a chlorine atom, instead of a third pathway yielding difluoroketene, photolysis can produce carbonylselenide, which forms molecular complexes with HCl.

Experimental Section

Preparation: Difluoroselenoacetic acid, $HCF_2C(O)SeH$, was prepared by treatment of $HCF_2C(O)OH$ with Woollins' reagent, $Ph_2P_2Se_4$, according to the reported procedure,[9] and purified by trap-to-trap fractional condensation in vacuo. Chlorodifluoroselenoacetic acid, $ClCF_2C(O)SeH$, was prepared in the same way from $ClCF_2C(O)OH$.[9]

Matrix Measurements: In each case, the pure compound (in a quantity of a few milligrams) was transferred into a small U-trap connected to the inlet nozzle of the matrix apparatus. A stream of Ar (2 mmol h^{-1}) was directed over the sample held at 158 K, and the resulting gas mixture was condensed under high vacuum onto the mirror plane of a rhodium-plated copper support held at 15 K. Photolysis experiments were performed with a high-pressure mercury lamp (TQ 150, Heraeus) using a water-cooled quartz lens optic. Schott filters were used to limit the lamp's output range. Details of the matrix apparatus are given elsewhere.[27] IR spectra of the Ar matrices were recorded in reflectance mode by means of a transfer optic using a Bruker IFS 66v spectrometer. An MCT-600 detector was used, together with a KBr/Ge beam splitter, in the region 5000–650 cm^{-1}. 100 scans were added for the spectra, with apodized resolutions of 0.5 and 0.15 cm^{-1}.

Theoretical Calculations: All quantum-chemical calculations were performed with the Gaussian 03 program package.[28] Second-order Møller–Plesset (MP2) and DFT B3LYP methods were employed using the 6-311++G** basis set. Geometries were optimized by standard gradient techniques with simultaneous relaxation of all geometric parameters.

Supporting Information (see footnote on the first page of this article): Theoretical geometrical parameters and vibrational frequencies of the *anti* and *gauche* conformers of HCF_2SeH (Tables S1 and S2) and $ClCF_2SeH$ (Tables S3 and S4) calculated with the B3LYP/6-311++G** and MP2/6-311++G**.

Acknowledgment

C. O. D. V. and R. M. R. thank the Consejo Nacional de Investigaciones Científicas y Técnicas (CONICET) (PIP 4695), the Agencia Nacional de Promoción Científica y Tecnológica (ANPCyT), the Comisión de Investigaciones Científicas de la Provincia de Buenos Aires (CIC), and the Facultad de Ciencias Exactas, UNLP for financial support. J. A. G. acknowledges an award from the Deutsche Akademische Austauschdienst (DAAD). C. O. D. V. especially acknowledges the DAAD, which generously supported the DAAD Regional Program of Chemistry of the Republic of Argentina, which encourages Latin-American students to perform their PhD work in La Plata.

[1] P. R. Schreiner, H. P. Reisenauer, D. Ley, D. Gerbig, C.-H. Wu, W. D. Allen, *Science* **2011**, *332*, 1300–1303.
[2] N. A. Young, *Coord. Chem. Rev.* **2013**, *257*, 956–1010.
[3] R. M. Romano, C. O. Della Védova, A. J. Downs, T. M. Greene, *J. Am. Chem. Soc.* **2001**, *123*, 5794–5801.
[4] R. M. Romano, C. O. Della Védova, A. J. Downs, *Chem. Eur. J.* **2007**, *13*, 8185–8192.

[5] B. R. Heazlewood, A. T. Maccarone, D. U. Andrews, D. L. Osborn, L. B. Harding, S. J. Klippenstein, M. J. T. Jordan, S. H. Kable, *Nature Chem.* **2011**, *3*, 443–448.

[6] J. A. Gómez Castaño, A. L. Picone, R. M. Romano, H. Willner, C. O. Della Védova, *Chem. Eur. J.* **2007**, *13*, 9355–9361.

[7] J. A. Gómez Castaño, R. M. Romano, H. Beckers, H. Willner, R. Boese, C. O. Della Védova, *Angew. Chem.* **2008**, *120*, 10268–10272; *Angew. Chem. Int. Ed.* **2008**, *47*, 10114–10118.

[8] J. A. Gómez Castaño, R. M. Romano, H. Beckers, H. Willner, C. O. Della Védova, *Inorg. Chem.* **2010**, *49*, 9972–9977.

[9] J. A. Gómez Castaño, R. M. Romano, H. Beckers, H. Willner, C. O Della Védova, *Inorg. Chem.* **2012**, *51*, 2608–2615.

[10] H. Dubost, *Chem. Phys.* **1976**, *12*, 139–151.

[11] R. M. Romano, A. J. Downs, *J. Phys. Chem. A* **2003**, *107*, 5298–5305.

[12] R. A. Hill, T. H. Edwars, *J. Chem. Phys.* **1965**, *42*, 1391–1396.

[13] D. E. Milligan, M. E. Jacox, *J. Chem. Phys.* **1968**, *48*, 2265–2271.

[14] A. Haas, H. Willner, H. Bürger, G. Pawelke, *Spectrochim. Acta Part A: Mol. Spectrosc.* **1977**, *33*, 937–945.

[15] C. Kötting, W. Sander, M. Senzlober, H. Bürger, *Chem. Eur. J.* **1998**, *4*, 1611–1615.

[16] D. E. Milligan, M. E. Jacox, J. H. McAuley, *J. Mol. Spectrosc.* **1973**, *45*, 377–403.

[17] R. M. Romano, C. O. Della Védova, A. J. Downs, *J. Phys. Chem. A* **2004**, *108*, 7179–7187.

[18] K. S. Rutkowxki, K. G. Tokhadze, P. Lipkowski, A. Koll, R. Ahmedjonov, M. Kulieva, *J. Mol. Struct.* **2001**, *598*, 205–211.

[19] L. Andrews, R. T. Arlinghaus, G. L. Johnson, *J. Chem. Phys.* **1983**, *78*, 6347–6352.

[20] K. S. Rutkowski, S. M. Melikova, *J. Mol. Struct.* **1999**, *511–512*, 233–240.

[21] H. Willner, *Z. Naturforsch. B Anorg. Chem. Org. Chem. B* **1984**, *39*, 314–316.

[22] C. O. Della Védova, H.-G. Mack, *Inorg. Chem.* **1993**, *32*, 948–950.

[23] P. D. Lightfoot, S. P. Kirwan, M. J. Pilling, *J. Phys. Chem.* **1988**, *92*, 4938–4946.

[24] R. C. Ferris, W. S. Haynes, *J. Am. Chem. Soc.* **1950**, *72*, 893–897.

[25] R. M. Romano, C. O. Della Védova, A. J. Downs, *J. Phys. Chem. A* **2002**, *106*, 7235–7244.

[26] E.-L. Hu, P.-Y. Tsai, H. Fan, K.-C. Lina, *J. Chem. Phys.* **2013**, *138*, 014302.

[27] H. Schnöckel, H. Willner, in: *Infrared and Raman Spectroscopy, Methods and Applications* (Ed.: B. Schrader), Wiley-VCH, Weinheim, Germany, **1994**, p. 297.

[28] M. J. Frisch, G. W. Trucks, H. B. Schlegel, G. E. Scuseria, M. A. Robb, J. R. Cheeseman, J. A. Montgomery Jr, T. Vreven, K. N. Kudin, J. C. Burant, J. M. Millam, S. S. Iyengar, J. Tomasi, V. Barone, B. Mennucci, M. Cossi, G. Scalmani, N. Rega, G. A. Petersson, H. Nakatsuji, M. Hada, M. Ehara, K. Toyota, R. Fukuda, J. Hasegawa, M. Ishida, T. Nakajima, Y. Honda, O. Kitao, H. Nakai, M. Klene, X. Li, J. E. Knox, H. P. Hratchian, J. B. Cross, C. Adamo, J. Jaramillo, R. Gomperts, R. E. Stratmann, O. Yazyev, A. J. Austin, R. Cammi, C. Pomelli, J. W. Ochterski, P. Y. Ayala, K. Morokuma, G. A. Voth, P. Salvador, J. J. Dannenberg, V. G. Zakrzewski, S. Dapprich, A. D. Daniels, M. C. Strain, O. Farkas, D. K. Malick, A. D. Rabuck, K. Raghavachari, J. B. Foresman, J. V. Ortiz, Q. Cui, A. G. Baboul, S. Clifford, J. Cioslowski, B. B. Stefanov, G. Liu, A. Liashenko, P. Piskorz, I. Komaromi, R. L. Martin, D. J. Fox, T. Keith, M. A. Al-Laham, C. Y. Peng, A. Nanayakkara, M. Challacombe, P. M. W. Gill, B. Johnson, W. Chen, M. W. Wong, C. Gonzalez, J. A. Pople, *Gaussian 03*, revision B.05, Gaussian, Inc., Wallingford CT, **2003**.

Received: March 8, 2013
Published Online: ■

